05,10

Nonlinear dynamics of a semi-infinite ferromagnet with the helicoidal structure

© V.V. Kiselev[1,2], A.A. Raskovalov[1,2,3,¶]

[1] M.N. Mikheev Institute of Metal Physics, Ural Branch, Russian Academy of Sciences, Yekaterinburg, Russia
[2] Ural Federal University after the first President of Russia B.N. Yeltsin, Institute of Physics and Technology (UrFU), Yekaterinburg, Russia
[3] Skolkovo Institute of Science and Technology, Moscow, Russia

¶ E-mail: raskovalov@imp.uran.ru

Received April 5, 2024
Revised September 6, 2024
Accepted September 16, 2024

For easy-plane ferromagnet without inversion center new types of solitons, built into the helicoidal structure of the semi-infinite sample, are found and analyzed, based on the Landau–Lifshitz model. The mixed boundary conditions are used. Their limiting cases correspond to free or completely pinned spins at the boundary of the sample. All chiral solitons are travelling. It is shown, that their cores near the surface of the sample are dramatically deformed. This process is accompanied by remagnetization of the medium. The dynamical properties of the chiral solitons and peculiarities of their elastic reflection from the edge of the sample are analyzed, depending on the character of pinning of the edge spins.

Keywords: solitons, Landau–Lifshitz equation, turning wave, easy-plane anisotropy, chiral breather.

DOI: 10.61011/PSS.2024.10.59628.150

1. Introduction

During last decade extensive attention is drawn to magnetic materials, which ground state is a helical structure. In crystals without the inversion center the helical ordering is frequently associated with Dzyaloshinskii–Moriya interaction, which is theoretically described by Lifshitz invariants in the free energy expansion [1–4]. Dzyaloshinskii–Moriya interaction competes with exchange interaction and turns spins relatively to each other by small angle. Many papers (see for example [5–11]) relate to study of the physical properties of materials with helicoidal structure. Detail summary of theory of uniaxial ferromagnets with helicoidal ground state is provided in paper [12].

When switching on external magnetic field perpendicular to axis of the helicoidal structure the magnetic spiral with constant pitch is converted into one-dimensional lattice of extended domains. Inside each of them the magnetization distribution is close to homogeneous. The neighboring domains are separated by narrow domain walls — topological solitons, where helical turn of magnetization is localized. The solitons comprising the lattice due to their mobility and magnetoresistive properties are promising for use in spintronics devices. Study of movement and stability of the soliton lattice and the single domain walls under the action of electric field is of great interest [13–16].

The helical ordering is implemented in rare-earth metals, in large class of conductive cubic magnetics without inversion center and in some other compounds. Among the known uniaxial helimagnets ($CrNb_3S_6$, $CrTaS_6$, CuB_2O_4, $CuCsCl_3$, $Yb(Ni_{1-x}Cu_x)_3Al_9$, $Ba_2CuGe_2O_7$) [17–22], $CrNb_3S_6$ is more extensively studied. The lattice of chiral solitons in it was observed in experiments [23].

The chiral multisolitons build into the helicoidal structure of the ferromagnets have useful technological properties [12,24]. But their analytical description is very complicated due to nonlinearity of the basic equations of the theory, and due to heterogeneity of helical ordering of the environment. Here we are taking about the study the collective particle-like excitations of helicoidal structure, which in the magnetic field orthogonal to the axis of magnetic spiral itself represents essentially nonlinear lattice of solitons. So far, there is a little number of studies relating this theme. The problem can be solved with use of simplified models, which correctly consider the basic interactions, and at the same time allow exact solutions. One of the models is a popular quasi-one-dimensional sine-Gordon equation. For infinite medium with homogeneous ground state it is completely integrable by the most effective method of nonlinear physics — by the method of inverse scattering problem. Presence of the non-trivial ground state complicates the construction particle like excitations even in the case of infinite medium. The simple chiral solitons in the lattice of solitons were obtained by Bäcklund transformation in the work [25]. The complete study of the multisolitons and spin waves in the helicoidal structure based on the method of inverse scattering problem in the framework of the sine–Gordon model is presented in the book [26] (see also [27,28]).

Another effective model of a chiral ferromagnet is associated with quasi-one-dimensional Landau–Lifshitz equations if the magnetic field is absent. Recall that during analysis of small amplitude wave spectrum in Heisenberg ferromagnet with Dzyaloshinskii interaction and the helical magnetic ordering with constant pitch the Landau–Lifshitz equation is frequently written in local benchmark, that shifts along the spiral axis (see, for example, [12] and works cited in it). Then in new reference frame the helical ordering corresponds to homogeneous distribution of magnetization, whereas the spin wave dynamics is described by linearized Landau–Lifshitz equation for a ferromagnet with exchange interaction without Dzyaloshinskii interaction, but with additional anisotropy of the „easy-plane" type. The works [5,26,29] established a deep relationship between exact solutions of significantly nonlinear Landau–Lifshitz model for a ferromagnet with the helicoidal structure taking into account the exchange energy, Dzyaloshinskii interaction and energy of quadratic in magnetization uniaxial anisotropy (the anisotropy axis is parallel to Dzyaloshinski vector), and the solutions of equivalent model of uniaxial ferromagnets without Dzyaloshinski interaction. The found relationship permits the use of soliton solutions of completely integrable equations of unbounded uniaxial ferromagnet with homogeneous ground state to construct and analyze the spin waves and non-trivial multisolitons (moving or in rest) in the ferromagnet with helicoidal structure. In general case, the presence of magnetization easy axis coinciding with the direction of Dzyaloshinskii vector suppresses the helicoidal ordering and keeps the metastable turn of magnetization in localized regions inside the sample only. For non-integrable one-dimensional Landau–Lifshitz equations this statement is justified by approximate methods in the works [15,16]. For integrable models of easy axis ferromagnets the formation of nuclei of chiral phase on the background of homogeneous distribution of magnetization is analytically described in [5,29]. On the contrary, the quadratic in magnetization easy-plane anisotropy (basis plane is parallel to plane of spin turn) keeps the helicoidal structure along full length of the sample. The particle-like solitons on the background of unbounded magnetic spiral are found and analyzed in [5,29].

The real samples have boundaries. Consideration of boundary conditions results in change of configuration of the helicoidal structure [12,30], and occurrence of important for applications features of dynamics of magnetic solitons and spin waves, which are absent in infinite medium. Besides, generalization of the method of inverse spectral transform on the samples with finite size faces to serious problems due to absence of simple mapping of the initial boundary conditions for Landau–Lifshitz models into the scattering data. Such representation is possible under special (integrable) boundary conditions only [31,32].

For finite ferromagnets without Dzyaloshinskii interaction the physically meaningful integrable conditions were established quite a while [33]. But nonlinear dynamics of finite samples, even without helicoidal structure till now is not studied because there is no effective scheme of inverse spectral transform for the finite systems. In the works [34,35] this problem was solved for the nonlinear Schrödinger equation by combination of the method of inverse scattering problem with „method of images", which is used in electrostatics when solving linear boundary problems with certain spatial symmetry. In the works [36–39] we used a scheme [34,35] to study solitons in the semi-infinite samples of Heisenberg ferromagnet and uniaxial ferromagnets with homogeneous ground state. In the present work we use these results for analytical description of the spin waves and solitons in the helicoidal structure of semi-infinite ferromagnet.

We succeeded generalize transformation of the works [5,29] and to establish relationship between solutions of the Landau–Lifshitz model for the semi-infinite uniaxial ferromagnet without Dzyaloshinskii interaction and the solutions of Landau–Lifshitz equations for the semi-infinite chiral ferromagnet at the boundary conditions corresponding to the partial pinning of spins at the boundary of sample. In combination with the method of integration of Landau–Lifshitz equations of semi-infinite ferromagnets with homogeneous ground state [37–39] the obtained transformation provides full analytical description of the multisolitons and dispersive waves in semi-infinite chiral ferromagnet with uniaxial magnetic anisotropy. Here we will discuss only the ferromagnet with anisotropy of the „easy-plane" type. Such type of the uniaxial anisotropy does not suppress the quasi-one-dimensional helicoidal structure in the sample bulk and results in non-trivial particle-like excitations on the background of magnetic spiral.

2. Semi-infinite ferromagnet with homogeneous ground state

Let's provide basic formulas for the semi-infinite ferromagnet with homogeneous ground state and homogeneous distribution of magnetization in sample depth [38,39], which are further used for the analytical description of solitons and waves in the helicoidal structure on half-axis $0 \le z < \infty$. Energy of such ferromagnet with anisotropy of the „easy-plane" type (plane Oxy) looks as follows [1]

$$E = \frac{1}{2}\int_0^\infty \mathrm{d}z \left[\alpha(\partial_z \mathbf{M})^2 + K(\mathbf{M}\cdot\mathbf{e}_3)^2\right] + H(\mathbf{M}\cdot\mathbf{e}_1)|_{z=0},$$

where $\mathbf{M}(z,t)$ — is the magnetization per unit of length along axis Oz ($\mathbf{M}^2 = M_0^2 = \mathrm{const}$), z and t — are the spatial coordinate and time, $\alpha > 0$ and $K > 0$ — are the constants of exchange interaction and anisotropy. Parameter H characterizes the effective field of unidirectional surface anisotropy $H = E_0/M_0$ caused by deposing the ferromagnetic layer on the surface of ferromagnetic sample [40–42]. Here E_0 — is the exchange energy per unit of surface of the sample. Its values for wide class of two-layer antiferromagnet–ferromagnet structures are given in [43]. Single vectors $\mathbf{e}_1 = (1, 0, 0)$ and $\mathbf{e}_3 = (0, 0, 1)$ specify the directions of the surface field and „hard axis" of magnetization, respectively.

In the dimensionless variables:

$$\mathbf{m} = -\mathbf{M}/M_0, \quad z' = z\sqrt{K/\alpha},$$

$$t' = \gamma M_0 K t, \quad h' = HM_0^{-1}/\sqrt{\alpha K}, \tag{1}$$

where γ — is magnetomechanical ratio, system energy is

$$E' = \frac{E}{M_0^2\sqrt{\alpha K}} = \frac{1}{2}\int_0^\infty \mathrm{d}z'[(\partial_{z'}\mathbf{m})^2 + m_3^2] - h'm_1|_{z=0}.$$

Possible nonlinear excitations in semi-infinite sample correspond to the solutions of the Landau–Lifshitz equation [26,44,45]:

$$\partial_{t'}\mathbf{m} = [\mathbf{m} \times \partial_{z'}^2\mathbf{m}] - (\mathbf{e}_3 \cdot \mathbf{m})[\mathbf{m} \times \mathbf{e}_3],$$

$$\mathbf{m}^2 = 1, \quad 0 \le z < \infty, \tag{2}$$

with integrable boundary conditions

$$[\mathbf{m} \times (\partial_{z'}\mathbf{m} + \mathbf{e}_1 h')]|_{z=0} = 0, \tag{3}$$

$$\mathbf{m} \to (1, 0, 0), \quad \partial_{z'}\mathbf{m} \to 0 \quad \text{at} \quad z' \to +\infty \tag{4}$$

and initial distribution of magnetization

$$\mathbf{m}(z', t' = 0) = \mathbf{m}_0(z'). \tag{5}$$

Selection of asymptotic boundary condition (4) corresponds to minimum of density of medium energy at $z' \gg 1$. Initial perturbation (5) is in agreement with conditions (3), (4). „Primes“ above the dimensionless variables are further omitted.

The mixed boundary condition (3) at $h \to 0$ transforms into the boundary condition of the problem with free surface spins [45]:

$$[\mathbf{m} \times \partial_z \mathbf{m}]|_{z=0} = 0.$$

In limit $|h| \to \infty$ it comes down to the condition of full pinning of spins at the sample boundary:

$$m_1|_{z=0} = \pm 1. \tag{6}$$

Sign selection in the right-hand part of (6) depends on the type of the solitons [38,39]. It will be clarified during further analysis.

The soliton evolution near the sample boundary can be formally treated as a result of interaction between the real soliton inside the sample and the fictive soliton of image outside the sample. During interaction with the sample surface in the soliton localization region the magnetization shifts and turns occur by the value of about saturation magnetization. Scenarios of solitons reflection depend on the degree of pinning of boundary spins. After reflection from the sample surface and by movement into the medium all solitons restore stationary shape, typical for solitons of the infinite medium.

In the works [38,39] it is shown that solitons of the semi-infinite easy-plane ferromagnet are divided into two classes. The first class includes the solitons which cores upon movement away from the sample boundary undertake the shape of waves of stationary profile without internal oscillations of magnetization. Such solitons can not be motionless. The magnetization distribution in the simplest of them looks like

$$m_1 = -1 + 2\tanh^2\rho(1 - n_1n_2)^2 d^{-1},$$

$$m_2 = -2\tanh^2\rho(n_1 + n_2)(1 - n_1n_2)d^{-1},$$

$$m_3 = 2\sinh\rho(n_2 - n_1)(1 - n_1n_2)/(d\cosh^2\rho),$$

$$d = (n_1 - n_2)^2 + (1 + n_1n_2)^2\tanh^2\rho,$$

$$n_1 = c_0 \exp\left(-\frac{z}{\cosh\rho} + \frac{\sinh\rho}{\cosh^2\rho}\,t\right),$$

$$n_2 = \frac{f}{c_0}\exp\left(-\frac{z}{\cosh\rho} - \frac{\sinh\rho}{\cosh^2\rho}\,t\right), \; f = \frac{h\cosh\rho + 1}{h\cosh\rho - 1}, \tag{7}$$

where c_0 — is real constant of integration, $-\infty < \rho < \infty$ — solution parameter. Next, for certainty, we consider $\rho > 0$. As befits, the solution (7) meets the boundary conditions (3), (4).

In weak surface fields $|h| < \cosh^{-1}\rho$ the parameter $f < 0$, and, vice versa, $f > 0$ at $|h| > \cosh^{-1}\rho$. It is manifested in various scenarios of deformation of soliton core (7) during interaction with the sample boundary, and results in differences in its steady profile in sample depth before and after reflection from surface. In both cases all spins inside the soliton are inclined to the sample boundary at $c_0 > 0$ or into the medium at $c_0 < 0$.

Let's explain the statement on the example of weak fields $|h| < \cosh^{-1}\rho$. Then, the detailed form of the solution (7):

$$m_1 = -1 + \frac{2}{\tau}\tanh^2\rho\cosh^2 y, \; y = \frac{z}{\cosh\rho} - \frac{1}{2}\log|f|,$$

$$m_2 = -\frac{2\operatorname{sgn} c_0}{\tau}\tanh^2\rho\sinh s\cosh y,$$

$$s = \frac{\sinh\rho}{\cosh^2\rho}(t - t_0), \quad t_0 = \frac{\cosh^2\rho}{2\sinh\rho}\log\frac{|f|}{c_0^2},$$

$$m_3 = -\frac{2\operatorname{sgn} c_0}{\tau\cosh^2\rho}\sinh\rho\cosh s\cosh y,$$

$$\tau = \cosh^2 s + \tanh^2\rho\sinh^2 y \tag{8}$$

immediately shows that at the moment t_0 of soliton (8) collission with boundary of sample all spins in the soliton localization region lay into the plane Oxz. The magnetization distribution in the plane Oxz depends on the sign of h. In negative fields $-\cosh^{-1}\rho < h < 0$ the magnetization component $m_1(z, t = t_0)$ monotonically increases with movement away from the edge $z = 0$ into the sample. In point $z = 0$ at rather high values $\rho >$ Arcsinh 1 the projection $m_1(z = 0, t = t_0)$ is positive. In this case the component $m_3(z, t = t_0)$ along full length of the sample also behaves monotonically, and magnetization in the soliton at the moment of collision with the boundary turns in the plane Oxz by angle lower than 90° (see Figure 1, *a*).

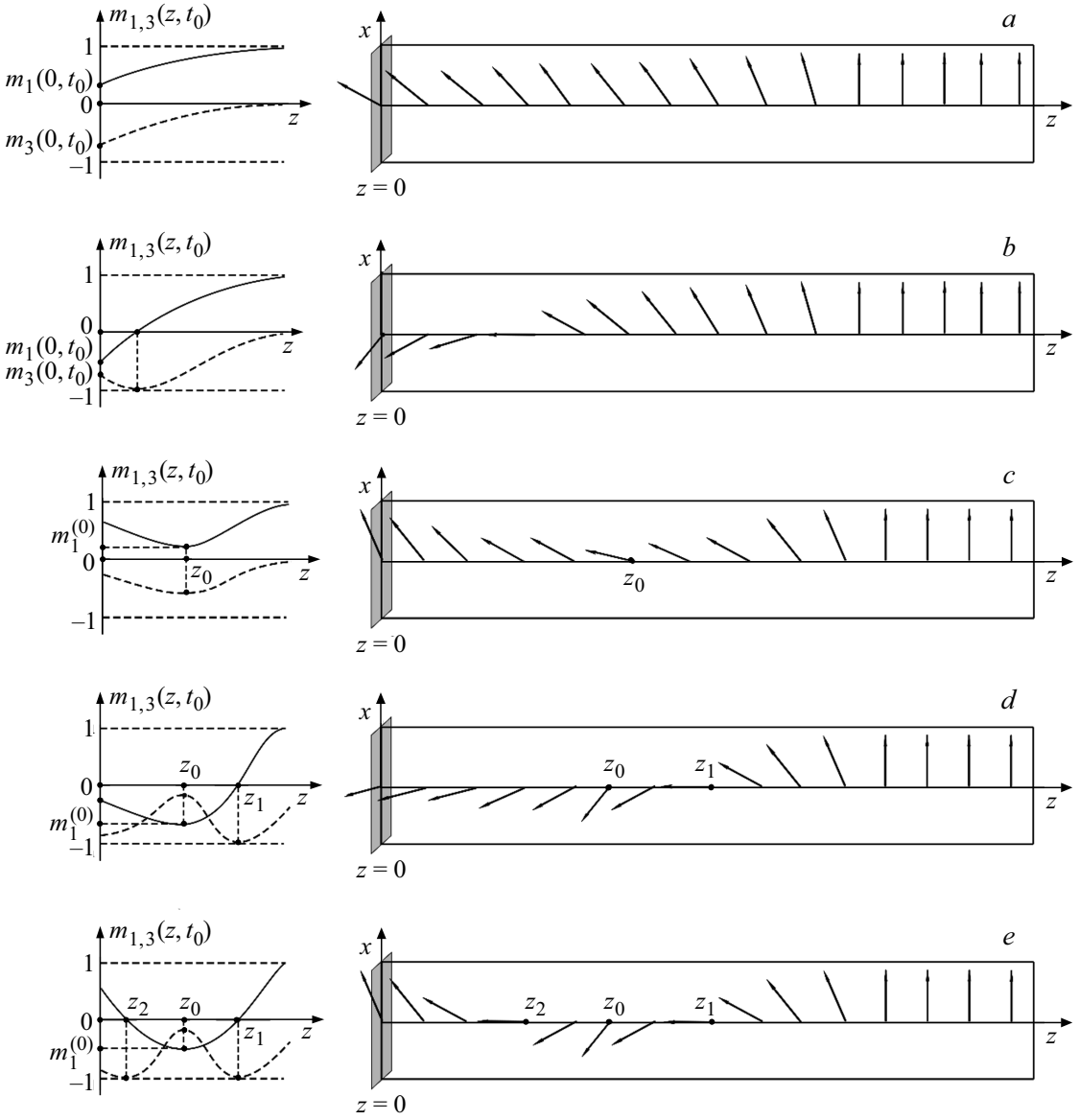

Figure 1. Magnetization components $m_1(z,t_0)$ (solid line), $m_3(z,t_0)$ (dashed line) of soliton (8) and spins distribution at time moment $t=t_0$ at values *a*) $-\cosh^{-1}\rho < h < 0$, $\rho > \mathrm{Arcsinh}1$; *b*) $-\cosh^{-1}\rho < h < 0$, $\rho < \mathrm{Arcsinh}1$; *c*) $0 < h < \cosh^{-1}\rho$, $\rho > \mathrm{Arcsinh}1$; *d*) $0 < h < \cosh^{-1}\rho\sqrt{1-\sinh^2\rho}$, $\rho < \mathrm{Arcsinh}1$; *e*) $\cosh^{-1}\rho\sqrt{1-\sinh^2\rho} < h < \cosh^{-1}\rho$, $\rho < \mathrm{Arcsinh}1$. In all cases $c_0 > 0$ was selected.

At relatively low values of $\rho < \mathrm{Arcsinh}1$ the projection $m_1(z, t=t_0)$ changes sign from minus to plus when crossing the point determined by the condition $\cosh y \sinh\rho = 1$, whereas the component $m_3(z, t=t_0)$ at this point has absolute minimum: $m_3 = -1$ (Figure 1, *b*).

In positive fields $0 < h < \cosh^{-1}\rho$ near the sample boundary at the point $z_0 = \cosh\rho \log|f|/2 > 0$ partial remagnetization of the medium occurs: $m_1^{(0)} = -1 + 2\tanh^2\rho$. The component $m_1(z, t=t_0)$ has a single minimum at the point z_0. As for the component $m_3(z, t=t_0)$, depending on ratio of values of parameter ρ and value of surface field it can have only one ($z = z_0$), two ($z = z_0$ and $z = z_1$), or even three points of extremum ($z = z_0$ and $z = z_{1,2}$). Appropriate cases are shown in Figure 1, *c*–*e*. Additional points $z_{1,2}$ — are zeros of function $m_1(z, t=t_0)$, determined by equality $\cosh[y(z_{1,2})]\sinh\rho = 1$.

Far from sample surface at $z \gg 1$ in limit $t \to \pm\infty$ the solution (8) undertakes shape of wave of stationary profile:

$$m_1 = \tanh\xi_\pm, \quad m_2 = \mp\mathrm{sgn}\, c_0 \frac{\tanh\rho}{\cosh\xi_\pm},$$

$$m_3 = -\frac{\mathrm{sgn}\, c_0}{\cosh\rho\cosh\xi_\pm},$$

$$\xi_\pm = (z \mp Vt - z_\pm)/l_0; \quad z_+ = \cosh\rho\log(|c_0|/\tanh\rho),$$

$$z_- = -\cosh\rho\log(|c_0|\tanh\rho/|f|), \qquad (9)$$

which is localized in region with width $l_0 = \cosh\rho > 1$ and moves with speed $V = \tanh\rho > 0$ inside the sample or

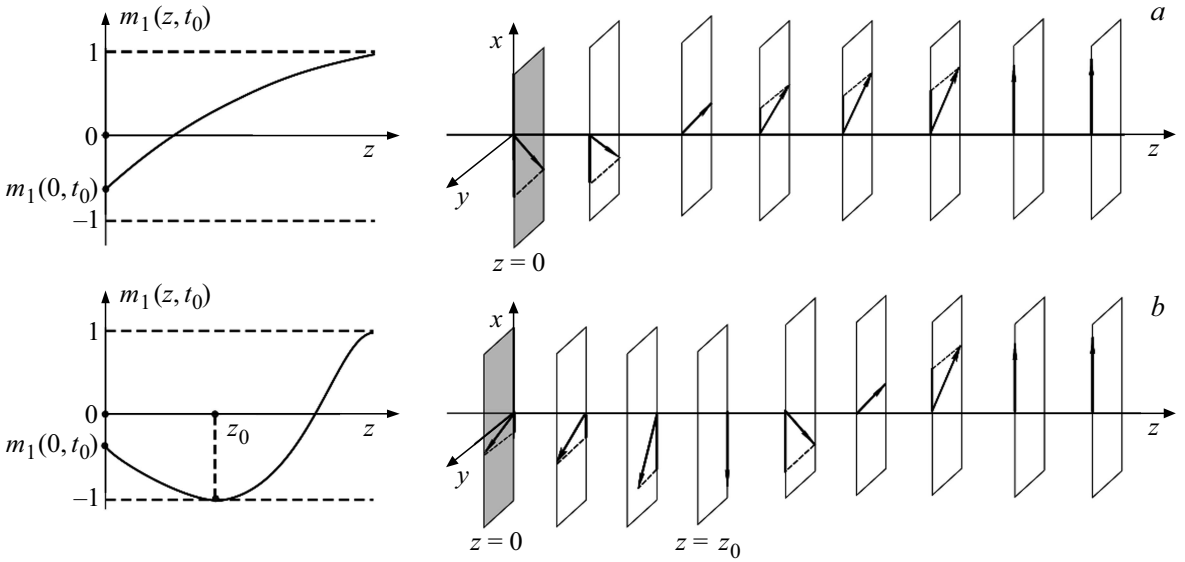

Figure 2. Magnetization component $m_1(z,t_0)$ of soliton (7) and distribution of spins at time moment $t=t_0$ at field values *a*) $h<-\sqrt{2}\cosh^{-1}\rho$ and *b*) $h>\sqrt{2}\cosh^{-1}\rho$; in both cases $c_0>0$ was selected.

towards its surface, parameters $z_\pm$ determine the coordinate of the wave center in co-moving reference frame, where $z\mp Vt=0$. This is the typical soliton of infinite easy-plane ferromagnet known as turning wave of magnetization [46,26]. The name is associated with that in wave localization region the magnetization turns by 180° from the position $\mathbf{m}=(-1,0,0)$ in soliton tail where $\xi_\pm\ll-1$, to the position $\mathbf{m}=(1,0,0)$ in its head, where $\xi_\pm\gg1$. At that in the soliton localization region the projection of vector $\mathbf{m}$ on plane Oyz forms the constant angle with axis Oz. The magnetization orientation in the center of the turning wave after and before the reflection is determined by the formulas

$$\mathbf{m}=(0,\sin\delta_\pm,\cos\delta_\pm),\ \sin\delta_\pm=\mp\mathrm{sgn}\,c_0\tanh\rho,$$

$$\cos\delta_\pm=-\mathrm{sgn}\,c_0/\cosh\rho.$$

As a result of the turning wave reflection from sample edge its center position shifts by the value Δz:

$$\Delta z=z_+-z_-=\cosh\rho\log(c_0^2/|f|). \tag{10}$$

From here we find the time of interaction of soliton (8) and sample surface: $|t-t_0|\le\Delta z/V$. Besides, the magnetization in the center of the soliton (8) after its collision with the boundary turns by angle

$$\delta_+-\delta_-=2\arg[1+i\sinh\rho]=2\arctan\sinh\rho. \tag{11}$$

In strong fields at $|h|>\cosh^{-1}\rho$ the soliton (7) is described by the expression obtained from (8) by formal replacements:

$$|f|\to f>0,\quad \cosh y\leftrightarrow\sinh y,\quad \sinh s\leftrightarrow\cosh s.$$

The expressions for y, s stay the same. Taking into account this remark, it is easy to establish that in strong fields the soliton (7) reflection from the sample edge occurs in another plane Oxy. At negative fields $h<-\cosh^{-1}\rho$ at the moment $t=t_0$ of collision with sample boundary the component m_1 of magnetization while moving into the sample steadily increases. At sample boundary $z=0$ the projection $m_1(z=0,t=t_0)$ is positive at values of field $-\sqrt{2}\cosh^{-1}\rho<h<-\cosh^{-1}\rho$ and negative at $h<-\sqrt{2}\cosh^{-1}\rho$. The last case is shown in Figure 2, *a*.

At positive values of $h>\cosh^{-1}\rho$ in the point $z_0=\cosh\rho(\log f)/2$, opposite to the case of small fields (8), complete remagnetization of medium is observed: $m_1=-1$. The projection $m_1(z=0,\ t=t_0)$ at the sample boundary is negative at $h>\sqrt{2}\cosh^{-1}\rho$ (Figure 2, *b*) and positive at $\cosh^{-1}\rho<h<\sqrt{2}\cosh^{-1}\rho$.

In Figure 2, *a*, *b* $c_0>0$ is selected. At $c_0<0$ direction of magnetization turning in plane Oxy will be inverse.

At $h>\cosh^{-1}\rho$ far away the sample boundary at $z\gg1$, $t\to\pm\infty$ the soliton (7) converts into the turning wave similar to (9):

$$m_1=\tanh\xi_\pm,\quad m_2=-\mathrm{sgn}\,c_0\frac{\tanh\rho}{\cosh\xi_\pm},$$

$$m_3=\mp\frac{\mathrm{sgn}\,c_0}{\cosh\rho\cosh\xi_\pm},$$

$$\xi_\pm=[z\mp Vt-z_\pm]/l_0,\quad z_+=\cosh\rho\log(|c_0|/\tanh\rho),$$

$$z_-=-\cosh\rho\log(|c_0|\tanh\rho/f). \tag{12}$$

Comparison of formulas (9) and (12) leads to the conclusion that in strong fields h the magnetization in center of soliton (7) after its collision with the sample boundary tuns in the plane Oyz by another angle:

$$\delta_+-\delta_-=\pi+2\arctan\sinh\rho, \tag{13}$$

which differs from previous angle (11) by π. Shift in soliton position is determined by the previous formula (10).

So, phase change of the complex field $m_3 + im_2$ in center of the turning wave after its reflection from the sample edge in the case of weak $|h| < \cosh^{-1}\rho$ and strong $|h| > \cosh^{-1}\rho$ surface fields is similar to the phase change of light wave during its reflection from the boundary with less and more optically dense medium. In next Section we show that changes of soliton cores (7) after their reflection from the sample boundary which have a threshold by amplitude of field h, are also take place for the chiral turning waves in the helicoidal structure. Features of medium remagnetization during chiral waves collision with the sample edge differ from those discussed here in only additional helical rotation of spins in region of soliton cores.

The second class of possible nonlinear excitations in the system represents pulsing solitons — breathers [38,39]. Inside the sample they elastically collide with each other and with turning waves of magnetization. The breathers reflection from the sample boundary is also elastic and accompanied by strong deformation of the soliton cores. At far distance from sample surface (at $z \gg 1$, $t \to \pm\infty$) the breather oscillations become regular, and it is converted into the precessing breather of the infinite medium [26]:

$$m_1 = 1 - \frac{2}{\tau_\pm}\left[\cos^2 s_\pm + \frac{\cos^2\varphi}{|\sinh\mu|^2}\right];$$

$$m_2 = \pm\frac{\cot\varphi}{\tau_\pm|\sinh\mu|^2} \times \left[\cos s_\pm \cosh y_\pm \sinh 2\rho - \sin s_\pm \sinh y_\pm \sin(2\varphi)\right],$$

$$m_3 = \frac{2\cot\varphi}{\tau_\pm|\sinh\mu|^2}\left[\sinh\rho\cos\varphi\cosh y_\pm \sin s_\pm + \cosh\rho\sin\varphi\sinh y_\pm\cos s_\pm\right], \qquad (14)$$

where

$$y_\pm = [z \mp Vt - z_\pm^{(0)}]/l_0, \quad s_\pm = kz \mp \omega t + s_\pm^{(0)},$$

$$\tau_\pm = \cos^2 s_\pm + \cot^2\varphi\cosh^2 y_\pm.$$

The soliton (14) is parametrized by complex value $\mu = \rho + i\varphi$; $-\infty < \rho < \infty$, $0 < \varphi < \pi$. Values

$$l_0 = \left(\frac{\cosh\rho\sin\varphi}{|\sinh\mu|^2}\right)^{-1} > 0, \quad V = \frac{\tanh\rho(\cosh^2\rho + \cos^2\varphi)}{|\sinh\mu|^2},$$

$$\omega = \frac{\cosh\rho\cos\varphi}{|\sinh\mu|^4}(\sinh^2\rho - \sin^2\varphi), \quad k = \frac{\sinh\rho\cos\varphi}{|\sinh\mu|^2}$$

respectively determine the thickness of walls limiting the breather core, movement speed of soliton center, frequency and wave number of oscillations in its core. Within soliton core (14) the magnetization performs inhomogeneous elliptical precessing with frequency ω around the axis Ox. The precession ellipse is elongated along the easy-plane Oxy. The precession cone pulses with frequency 2ω. This results in longitudinal oscillations of soliton size. The only result of the breather (14) reflection from the sample boundary is shift of its center

$$z_+^{(0)} = l_0\log\left|\frac{\kappa}{\tanh\rho\coth\mu}\right|, \quad z_-^{(0)} = l_0\log\left|\frac{f}{\kappa\tanh\rho\coth\mu}\right|,$$

$$f = \frac{ih\sinh\mu + 1}{ih\sinh\mu - 1}$$

and change of initial phase of its precession:

$$s_+^{(0)} = \arg\left[\tanh\rho\coth\mu\,\kappa^{-1}\right], \quad s_-^{(0)} = \arg\left[\kappa\tanh\rho\coth\mu\, f^{-1}\right].$$

Unlike the case of infinite medium, the breather on half-axis, like the turning wave, can not be motionless ($\rho \neq 0$, $V \neq 0$).

We have shown that in limit $|h| \to \infty$ the solution of initial boundary value problem (2), (3) for the semi-infinite sample, comprising N turning waves of magnetization and arbitrary number of breathers and dispersive spin wave packets, transforms into the solution of the same model at the boundary conditions

$$\mathbf{m}(z=0,t) \to (-1)^N\mathbf{e}_1; \quad \mathbf{m}(z,t) \to \mathbf{e}_1;$$

$$\partial_z\mathbf{m}(z,t) \to 0 \quad \text{at} \quad z \to +\infty.$$

At positive (negative) finite values of the surface field the formation on the half-axis of even (odd) number of turning waves is more beneficial by the energy. It follows from this that formation of odd or even number of waves in the system can be regulated changing nature of spins pinning at the boundary. This conclusion is true also for the chiral turning waves.

At weak external influences in the sample only dispersive waves without solitons are formed. In case of small amplitude spin waves the magnetization in semi-infinite sample is described by the expressions [38,39]:

$$m_3 = -\frac{2}{\pi}\,\mathrm{Im}\left[\int_0^{+\infty} d\xi\,\frac{b_0(\xi)}{\sinh\xi}\,\exp\left(\frac{it\cosh\xi}{\sinh^2\xi}\right) \times \mathrm{Re}\left(\frac{\exp(iz\sinh^{-1}\xi)}{\sinh^{-1}\xi + ih}\right)\right], \; m_1 \approx 1;$$

$$m_2 = \frac{2}{\pi}\,\mathrm{Re}\left[\int_0^{+\infty} d\xi b_0(\xi)\coth\xi\exp\left(\frac{it\cosh\xi}{\sinh^2\xi}\right) \times \mathrm{Re}\left(\frac{\exp(iz\sinh^{-1}\xi)}{\sinh^{-1}\xi + ih}\right)\right]. \qquad (15)$$

where b_0 is the inverse scattering problem coefficient corresponding to presence of dispersive waves [26].

By direct check we easily make sure that (15) is the solution of the linearized Landau–Lifshitz equation (2):

$$\partial_t m_2 + \partial_z^2 m_3 - m_3 = 0, \quad \partial_t m_3 - \partial_z^2 m_2 = 0,$$

$$|m_{2,3}| \ll 1, \quad 0 < z < +\infty$$

with linearized boundary conditions (3), (4):

$$(\partial_z m_{2,3} - h\,m_{2,3})|_{z=0} = 0, \; m_{2,3} \to 0 \quad \text{at} \quad z \to +\infty.$$

3. Solitons of semi-infinite ferromagnet with helicoidal structure

Let's consider quasi-one-dimensional ferromagnetic crystal without inversion center with energy density:

$$w = \frac{\alpha}{2}(\partial_z \mathbf{M})^2 + \frac{KM_3^2}{2} - \kappa(M_1\partial_z M_2 - M_2\partial_z M_1).$$

Here we use previous marks for medium magnetization $\mathbf{M}(z,t)$ ($\mathbf{M}^2 = M_0^2 = \text{const}$), spatial coordinate $0 < z < \infty$, time t, constants of exchange interaction $\alpha > 0$ and easy-plane anisotropy $K > 0$. Besides, we consider the Dzyaloshinskii interaction, to which Lifshitz invariant corresponds

$$-\kappa(M_1\partial_z M_2 - M_2\partial_z M_1),$$

compatible with the uniaxial symmetry of the magnetic crystal without the inversion center. The constant κ can have any sign.

Now, the conditions $\alpha > 0$, $K > 0$ do not ensure stability of the homogeneous state of medium in sample depth (at $z \gg 1$). The most stable turns out to be inhomogeneous distribution of magnetization, that is, the helicoidal structure:

$$\mathbf{M} = -M_0(\cos(pz), \sin(pz), 0), \tag{16}$$

where $p = \kappa/\alpha$. Period of magnetic spiral $2\pi/|p|$ is much more than the crystallographic periods a: $2\pi\alpha/|\kappa| \gg a$ and usually incommensurable with them.

Let, as previously, along the boundary $z = 0$ of the sample we have the effective field of unidirectional surface anisotropy $\mathbf{H} = H\mathbf{e}_1$, where $\mathbf{e}_1 = (1, 0, 0)$. The helical ordering corresponds to energy density $-M_0^2\kappa^2/(2\alpha)$. We will take the system energy from the helicoidal ground state of the medium at $z \gg 1$. Then total energy of the sample will be written as follows

$$E = \frac{1}{2}\int_0^\infty \mathrm{d}z \left[\alpha(\partial_z \mathbf{M})^2 + KM_3^2 + \frac{M_0\kappa^2}{\alpha} - 2\kappa(M_1\partial_z M_2 - M_2\partial_z M_1)\right] + HM_1|_{z=0}. \tag{17}$$

Let's go to dimensionless variables:

$$\mathbf{m} = -\mathbf{M}/M_0, \quad \tilde{z} = z\left[\frac{1}{\alpha}\left(K + \frac{\kappa^2}{\alpha}\right)\right]^{1/2},$$

$$\tilde{t} = \gamma M_0 t\left(K + \frac{\kappa^2}{\alpha}\right), \quad \tilde{h} = \frac{H}{M_0}\left[\alpha\left(K + \frac{\kappa^2}{\alpha}\right)\right]^{-1/2},$$

which coincide with previous (1) at $\kappa = 0$. In new variables the system energy looks like

$$\tilde{E} = \frac{E}{M_0^2}\left[\alpha\left(K + \frac{\kappa^2}{\alpha}\right)\right]^{-1/2} = \frac{1}{2}\int_0^\infty \mathrm{d}\tilde{z}[(\partial_{\tilde{z}}\mathbf{m})^2 + (1-q^2)m_3^2 - 2q(m_1\partial_{\tilde{z}}m_2 - m_2\partial_{\tilde{z}}m_1) + q^2] - \tilde{h}\,m_1|_{\tilde{z}=0}.$$

Helical structure (16) corresponds field distribution $\mathbf{m}$:

$$\mathbf{m} = (\cos(q\tilde{z}), \sin(q\tilde{z}), 0), \tag{18}$$

where $q = \kappa/[\alpha(K + \kappa^2/\alpha)]$.

Possible nonlinear excitations of the helicoidal structure of semi-infinite ferromagnetic sample correspond to solutions of Landau–Lifshitz equation:

$$\partial_{\tilde{t}}\mathbf{m} = [\mathbf{m} \times \partial_{\tilde{z}}^2\mathbf{m}] - (1-q^2)(\mathbf{e}_3 \cdot \mathbf{m})[\mathbf{m} \times \mathbf{e}_3] + 2q(\mathbf{e}_3 \cdot \mathbf{m})\partial_{\tilde{z}}\mathbf{m}, \tag{19}$$

where $\mathbf{m}^2 = 1$, $0 < \tilde{z} < \infty$, with boundary conditions:

$$[\mathbf{m} \times (\partial_{\tilde{z}}\mathbf{m} + q[\mathbf{m} \times \mathbf{e}_3] + \tilde{h}\,\mathbf{e}_1)]|_{\tilde{z}=0} = 0,$$
$$\mathbf{m} \to (\cos(q\tilde{z}), \sin(q\tilde{z}), 0) \quad \text{at} \quad \tilde{z} \to +\infty \tag{20}$$

and a given initial perturbation of the helical structure:

$$\mathbf{m}(\tilde{z}, \tilde{t} = 0) = \mathbf{m}_0(\tilde{z}), \tag{21}$$

which is compatible with conditions (20). Vector $\mathbf{e}_3 = (0, 0, 1)$, like previously, specifies the direction of the „hard-axis" of magnetization.

To determine relationship between the problems (2)–(5) and (19)–(21) we will use parameterization of the normalized magnetization by angles Θ and Φ:

$$\mathbf{m} = (\cos\Theta\cos\Phi, \cos\Theta\sin\Phi, \sin\Theta).$$

Landau–Lifshitz equation (19) together with the boundary conditions (20) follows from Hamilton variation principle for action functional:

$$S = \int_0^\infty \mathrm{d}\tilde{z}\left(\sin\Theta\,\partial_{\tilde{t}}\Phi - \frac{1}{2}[(\partial_{\tilde{z}}\Theta)^2 + \cos^2\Theta(\partial_{\tilde{z}}\Phi - q)^2 + \sin^2\Theta]\right) + \tilde{h}\cos\Theta\cos\Phi|_{z=0}. \tag{22}$$

The initial boundary value problem (2)–(5) for the easy-plane ferromagnet with homogeneous ground state is described by action that follows from (22) at $q = 0$. From here the important statement follows, which represents generalization of established in [26,29] for infinite medium. If we know solution $\Theta^{(l)}(z,t,h)$, $\Phi^{(l)}(z,t,h)$ of Landau–Lifshitz equation (2) with boundary conditions (3) and (4), then the solution $\Theta^{(g)}(\tilde{z},\tilde{t},\tilde{h},q)$, $\Phi^{(g)}(\tilde{z},\tilde{t},\tilde{h},q)$ of model (19), (20) of chiral ferromagnet is determined by formulas

$$\Phi^{(g)}(\tilde{z},\tilde{t},\tilde{h},q) = \Phi^{(l)}(z = \tilde{z}, t = \tilde{t}, h = \tilde{h}) + q\tilde{z},$$
$$\Theta^{(g)}(\tilde{z},\tilde{t},\tilde{h},q) = \Theta^{(l)}(z = \tilde{z}, t = \tilde{t}, h = \tilde{h}).$$

After shown transformation the action functional of one problem transits into the functional of another problem. This justifies equivalence of not only equations, but also the initial boundary value conditions for two problems. Distributions

of magnetization $\mathbf{m}^{(l)}(z, t, h)$ and $\mathbf{m}^{(g)}(\tilde{z}, \tilde{t}, \tilde{h}, q)$ of these problems are related to each other:

$$m_+^{(g)}(\tilde{z}, \tilde{t}, \tilde{h}, q) = m_+^{(l)}(z = \tilde{z}, t = \tilde{t}, h = \tilde{h})\, \mathrm{e}^{iq\tilde{z}},$$

$$m_3^{(g)}(\tilde{z}, \tilde{t}, \tilde{h}, q) = m_3^{(l)}(z = \tilde{z}, t = \tilde{t}, h = \tilde{h}), \qquad (23)$$

where $m_+ = m_1 + im_2$. When comparing solutions (23) the interaction constants also change.

In particular, small-amplitude spin wave field in semi-infinite sample of the chiral ferromagnet looks like

$$\mathbf{m}^{(g)} = \mathbf{n} + \left(m_2^{(l)}[\mathbf{e}_3 \times \mathbf{n}] + m_3^{(l)}\mathbf{e}_3\right)|_{z=\tilde{z}, t=\tilde{t}, h=\tilde{h}},$$

$$\mathbf{n} = (\cos(q\tilde{z}), \sin(q\tilde{z}), 0), \qquad (24)$$

where functions $m_{2,3}^{(l)}$ are determined by formulas (23). By direct check we can easily make sure that expression (24) satisfies the linearized Landau–Lifshitz equation (19) with linearized boundary condition (20).

The turning wave (7) of the ferromagnet with homogeneous ground state after transformation (23) converts into the chiral turning wave in semi-infinite ferromagnet with same in the helical structure:

$$m_1^{(g)} = m_1^{(l)} \cos(q\tilde{z}) - m_2^{(l)} \sin(q\tilde{z}),$$

$$m_2^{(g)} = m_1^{(l)} \sin(q\tilde{z}) + m_2^{(l)} \cos(q\tilde{z}),\ m_3^{(g)} = m_3^{(l)}, \qquad (25)$$

where expressions $m_j^{(l)}$ are determined by formulas (7) after the replacements $z \to \tilde{z}$, $t \to \tilde{t}$, $h \to \tilde{h}$. At large distances from the sample edge the solution (25) describes the simplest soliton of infinite medium [26,29]. The magnetization in such soliton can be twisted either to the direction or against the direction of turning of magnetic spiral (18), which, respectively, results in decreasing or increasing the spiral pitch. Both are accompanied by exit of the magnetic moments from the plane Oxy.

Near the sample surface the core of the chiral soliton (25) strongly deforms, after this it elastically reflects from the sample boundary and restores its stationary shape. As result of reflection the center of chiral wave shifts by value Δz (10).

The chiral solitons inherit basic dynamic properties of solitons of Section 2.

Let's specify the made general remarks. We will suppose that the parameter $\rho > 0$. To simplify the analysis we assume that presence of soliton does not change direction of turning of spiral (18), and results only in decreasing or increasing its pitch. Then in case of weak surface anisotropy $|h| < \cosh^{-1}\rho$ at the value of integration constant $c_0 > 0$ ($c_0 < 0$) before the collision with the sample boundary in the localization region of soliton (25) the spiral pitch decreases (increases), and after collision — increases (decreases). At that along full length of sample at $c_0 > 0$ the spins are inclined towards the boundary, and at $c_0 < 0$ — from the boundary. During soliton reflection from the sample edge in its center the projection of magnetization

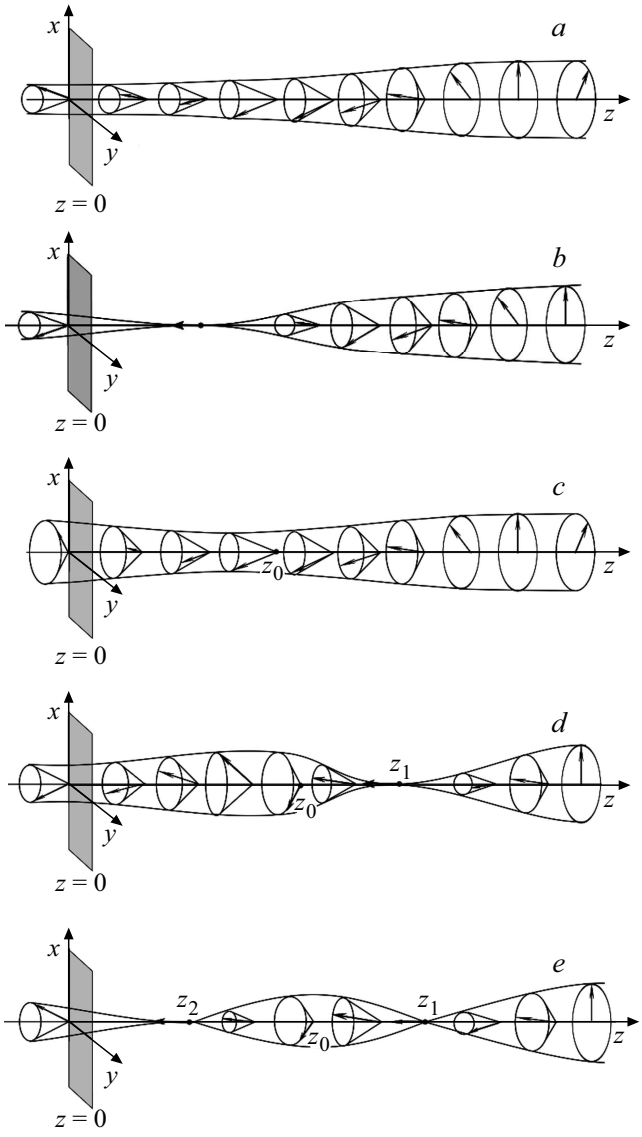

Figure 3. Spins location in soliton (25) at moment $t = t_0$ of collision with sample boundary at values *a*) $-\cosh^{-1}\rho < h < 0$, $\rho >$ Arcsinh1; *b*) $-\cosh^{-1}\rho < h < 0$, $\rho <$ Arcsinh1; *c*) $0 < h < \cosh^{-1}\rho$, $\rho >$ Arcsinh1; *d*) $0 < h < \cosh^{-1}\rho\sqrt{1 - \sinh^2\rho}$, $\rho <$ Arcsinh1; *e*) $\cosh^{-1}\rho\sqrt{1 - \sinh^2\rho} < h < \cosh^{-1}\rho$, $\rho <$ Arcsinh1. In all cases $c_0 > 0$ was selected.

$m_3^{(g)}$ on the spiral axis does not change (see formulas (9) and (25)). At the moment $t = t_0$ (see (8)) of soliton (25) collision with the sample boundary the spiral pitch and phase of spins turning within soliton exactly coincide with same in the helical structure helical structure (18), and soliton presence in the structure could be seen only by spins exit from the turning plane Oxy.

In weak negative fields $-\cosh^{-1}\rho < h < 0$ at rather high large values of $\rho >$ Arcsinh1 the magnetization component $m_3(z, t_0)$ is monotonous while moving into the sample. This means that in this case the envelope of the soliton at $t = t_0$ is most narrow in point $z = 0$ at the boundary of the

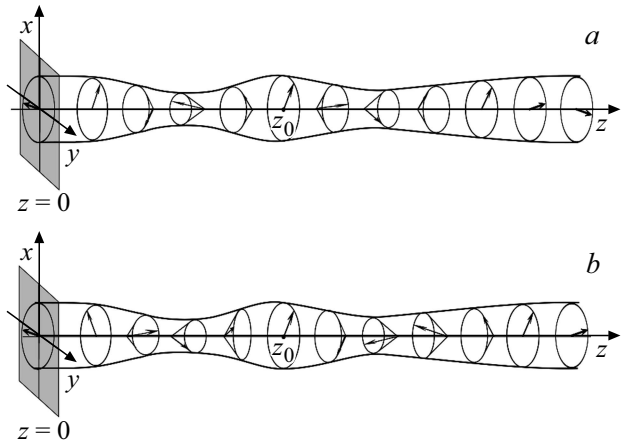

Figure 4. Spins location in soliton (25) in case of large positive fields $h > \cosh^{-1}\rho$ directly *a*) before and *b*) after collision with sample boundary; $c_0 > 0$ was selected. At the moment of collision the spins along the entire sample lay in plane Oxy.

sample (Figure 3, *a*). At relatively small $\rho <$ Arcsinh1 the projection $m_3^{(g)}$ reaches absolute minimum -1 in the point determined by the condition $\cosh y \sinh\rho = 1$ (Figure 3, *b*). In positive fields $0 < h < \cosh^{-1}\rho$ at rather large values $\rho >$ Arcsinh1 the magnetization component $m_3^{(g)}(z, t_0)$ has only one point of extremum $z_0 = \cosh\rho \log|f|/2 > 0$ near the boundary (Figure 3, *c*). The soliton envelope is compressed in the point $z = z_0$, and extends at both sides from the point z_0, gradually reaching the limiting value corresponding to the helicoidal structure (18). At relatively small $\rho <$ Arcsinh1 depending on values of field h the component $m_3^{(g)}(z, t_0)$ obtains one more or two additional points of absolute minimum $z_{1,2}$, determined by the condition $\cosh[y(z_{1,2})]\sinh\rho = 1$ (Figure 3, *d* and *e*). In these points the magnetization is parallel to the „hard-axis" of the bulk anisotropy: $\mathbf{m}^{(g)} = (0, 0, -1)$.

Cases in Figure 3, *a*–*e* are similar to those in Figure 1, *a*–*e*. Ranges of values of the surface field, given in text to Figure 3, *a*–*e*, exactly coincide with the same in Figure 1, *a*–*e*.

At strong surface anisotropy $|h| > \cosh^{-1}\rho$ the component $m_3^{(g)}$ in the center of soliton after the reflection changes the sign (see (12), (25)). This means that as results of interaction of soliton (25) with the sample boundary the tilt of spins towards the boundary or from the boundary changes to opposite (Figure 4, *a* and *b*). Just at the moment $t = t_0$ of soliton collision with the sample surface the magnetization component $m_3^{(g)} = 0$, and, hence, spins in the entire sample lay in plane Oxy. In soliton, built into the helical structure, the spins inclination (towards the sample boundary or from it) depends on sign of the parameters h and c_0 like in „seed" soliton in a ferromagnet with homogeneous ground state.

Note that unlike the case of small fields $|h| < \cosh^{-1}\rho$, in strong fields $|h| > \cosh^{-1}\rho$ the twisting direction of soliton (25) during reflection from the sample boundary does not change. In localization region of soliton the spiral pitch (18) at $c_0 > 0$ ($c_0 < 0$) both before, and after soliton collision with the sample boundary is increased (decreased) as compared to pitch of the helical structure (compare formulas (12), (18)).

As a conclusion let's discuss the chiral breather. The breather solution of the easy-plane ferromagnet [38,39] by means of transformation (25) transits into pulsing soliton on the background of helical structure (18). Figure 5, *a* and *b* schematically shows such soliton far from sample edge (at $z \gg 1$) at time moments $t = 0$ and $t = T/2$, where $T = 2\pi/\omega$ — is the period of pulsations. In center of soliton — point z_0 — the magnetization component $m_3^{(g)}$ reaches the extreme value, and the vector $\mathbf{m}^{(g)}(z, t)$ periodically changes inclination from the direction towards the sample boundary to the direction into the sample. In the soliton the stretching regions of the helical structure alternate with compression regions. In Figure 5, *a* at $t = 0$ to the right of the center of soliton (in region $z > z_0$) the helical structure is stretched, and to the left of the center (in region $z < z_0$) it is compressed. After half-period of oscillations, at $t = T/2$ (Figure 5, *b*) the spiral stretching at right of the center of soliton changes by its compression, and compression of spiral to the left of the center of soliton changes by stretching. At that the projection $m_3^{(g)}$ both to the right, and to the left of the center periodically changes the sign to opposite.

Besides, heterogeneity of the precession of magnetization and pulsations in the breather core result in small longitudinal oscillations of soliton along the axis of magnetic spiral. They are not shown in Figure 5.

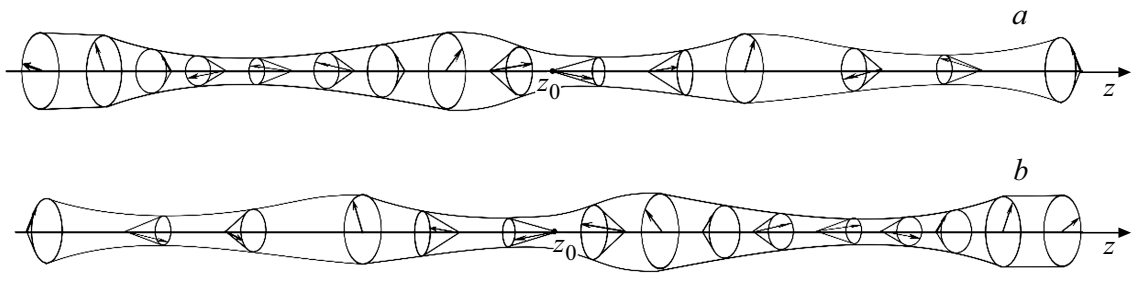

Figure 5. Spins location in pulsing soliton — breather — on background of helical structure (18) far from the sample boundary at time moments *a*) $t = 0$ and *b*) $t = T/2$, where T — is the period of pulsations.

4. Conclusion

Method of inverse scattering problem in combination with the special transformation of solutions of model of semi-infinite ferromagnet with the homogeneous ground state used to construct and analyze the new class of explicit solutions of Landau–Lifshitz equation describing spreading of dispersive waves and solitons along the helicoidal structure of the semi-infinite ferromagnet with anisotropy of the „easy-plane" type. At sample boundary the boundary condition was considered, that corresponds to partial pinning of the helicoidal structure. Its limiting cases correspond to free edge spins and complete pinning of magnetization at the sample boundary. Soliton-like nuclei of the helicoidal phase on the background of homogeneous distribution of magnetization in the semi-infinite ferromagnet with anisotropy of „easy axis" type can also be studied using the suggested approach. For this it is sufficient to use formulas of the work [37] for solitons in semi-infinite easy-axis ferromagnet with homogeneous ground state.

If Dzyaloshinskii interaction is absent the easy-plane ferromagnet has two classes of solitons. One of them comprises turning waves of magnetization, which remind the moving 180°-domain walls. Second type of solitons — pulsing solitons with magnetization precession near the „easy-plane". Dzyaloshinskii interaction ensures the formation of the helicoidal structure and built-in solitons. It is important that chiral solitons are inseparable from the helical structure. They inherit some features of solitons of the ferromagnet with homogeneous ground state and obtain new features. The turning waves with different turning of magnetization on the background of homogeneous state of medium have same energy, but corresponding to them chiral turning waves significantly differ in core structure, and hence, in energy. The energy of the magnetic soliton in the helicoidal structure shall mean the difference between the energy of system with soliton in it and energy of helicoidal ground state of medium without soliton. The correct calculation of such energy is a theme of separate study. Dependence of energy of chiral solitons on the parameters of the helicoidal structure and surface anisotropy shall be considered, for example, when describing the thermodynamic properties of solitons system in semi-infinite sample.

It is establshed that structure of chiral turning waves (7), (25) after reflection from the sample surface depends in threshold manner on the amplitude of the surface field h. Besides, „deformation" of soliton core at the moment of the collision with the sample surface significantly depends on sign of h. The chiral breathers, unlike the chiral turning waves, have characteristic frequencies of internal pulsations. So, the breathers can be detected by the resonance absorption of energy at frequencies of their oscillations.

All types of solitons in the helicoidal structure are moving particle-like objects. The experimental confirmation of peculiarities of their elastic reflection from sample boundary obtained during study is actual.

Collision of chiral solitons with sample surface is accompanied by significant change in their internal structure and dynamic properties, and also by processes of medium remagnetization by the value about saturation magnetization. So, the chiral solitons in semi-infinite sample can not be described by the traditional method of perturbation theory for infinite medium. This theory supposes sufficient „hardness" of soliton cores and small changes of their properties under influences of perturbations.

The study results shall be considered during modeling of soliton processes near surface of real ferromagnets with helicoidal structure. The obtained analytical solutions are useful for numerical calculations verification.

Funding

This study was carried out as part of project of RSF No. 19-72-30028.

Conflict of interest

The authors declare that they have no conflict of interest.

References

[1] L.D. Landau, E.M. Lifshitz, L.P. Pitaevskii. Landau and Lifshitz Course of Theoretical Physics. Volume 8. Electrodynamics of Continuous Media. Elsevier Science (1995).
[2] I.E. Dzyaloshinskii. Sov. Phys. JETP **20**, *3*, 665 (1965).
[3] T. Moriya. Phys. Rev. **120**, *1*, 91 (1960).
[4] Yu.A. Izyumov. Sov. Phys. Usp. **27**, *9*, 845 (1984).
[5] Yu.A. Izyumov. Difraktsiaya neitronov na dlinnoperiodicheskih strukturah. Energoatomizdat, M. (1987). S. 180–181.
[6] V.D. Buchel'nikov, I.V. Bychkov, V.G. Shavrov. J. Magn. Magn. Mater. **118**, *1–2*, 169 (1993).
[7] A.A. Fraerman, O.G. Udalov. Phys. Rev. B **77**, *9*, 094401 (2008).
[8] I.V. Bychkov, D.A. Kuzmin, V.G. Shavrov. J. Magn. Magn. Mater. **329**, 142 (2013).
[9] A.A. Tereshchenko, A.S. Ovchinnikov, I. Proskurin, E.V. Sinitsyn, J. Kishine. Phys. Rev. B **97**, *18*, 184303 (2020).
[10] J. Kishine, A.S. Ovchinnikov. Phys. Rev. B **101**, *18*, 184425 (2020).
[11] Yu.B. Kudasov. Phys. Solid State **65**, *6*, 898 (2023).
[12] J. Kishine, A.S. Ovchinnikov. Solid State Phys. **66**, 1 (2015).
[13] J. Kishine, A.S. Ovchinnikov, I.V. Proskurin. Phys. Rev. B **82**, 064407 (2010).
[14] K. Tokushuku, J. Kishine, M. Ogata. J. Phys. Soc. Jpn. **86**, *12*, 124701 (2017).
[15] V. Laliena, S. Bustingorry, J. Campo. Sci. Rep. **10**, *1*, 20430 (2020).
[16] S.A. Osorio, A. Athanasopoulos, V. Laliena, J. Campo, S. Bustingorry. Phys. Rev. B **106**, *9*, 094412 (2022).
[17] K. Adachi, N. Achiwa, M. Mekata. J. Phys. Soc. Jpn. **49**, *2*, 545 (1980).
[18] A. Zheludev, S. Maslov, G. Shirane, Y. Sasago, N. Koide, K. Uchinokura. Phys. Rev. Lett. **78**, *25*, 4857 (1997).
[19] B. Roessli, J. Schefer, G.A. Petrakovskii, B. Ouladdiaf, M. Boehm, U. Staub, A. Vorotinov, L. Bezmaternikh. Phys. Rev. Lett. **86**, *9*, 1885 (2001).

[20] S. Ohara, S. Fukuta, K. Ohta, H. Kono, T. Yamashita, Y. Matsumoto, J. Yamaura. JPS Conf. Proc. **3**, 017016 (2014).
[21] Y. Kousaka, T. Ogura, J. Zhang, P. Miao, S. Lee, S. Torii, T. Kamiyama, J. Campo, K. Inoue, J. Akimitsu. J. Phys.: Conf. Ser. **746**, *1*, 012061 (2016).
[22] T. Matsumura, Y. Kita, K. Kubo, Y. Yoshikawa, S. Michimura, T. Inami, Y. Kousaka, K. Inoue, S. Ohara. J. Phys. Soc. Jpn. **86**, *12*, 124702 (2017).
[23] Y. Togawa, T. Koyama, K. Takayanagi, S. Mori, Y. Kousaka, J. Akimitsu, S. Nishihara, K. Inoue, A.S. Ovchinnikov, J. Kishine. Phys. Rev. Lett. **108**, *10*, 107202 (2012).
[24] A.B. Borisov, V.V. Kiselev. Dvumernye i trekhmernye magnitnye topologicheskie defekty, solitony i tekstury v magnetikakh. Fizmatlit, M. (2022), 456 s. (in Russian).
[25] A.B. Borisov, J. Kishine, I.G. Bostrem, A.S. Ovchinnikov. Phys. Rev. B **79**, *13*, 134436 (2009).
[26] A.B. Borisov, V.V. Kiselev. Kvaziodnomernye magnitnye solitony. Fizmatlit, M. (2014). 520 s. (in Russian).
[27] V.V. Kiselev, A.A. Raskovalov. JETP **116**, *2*, 272 (2013).
[28] V.V. Kiselev, A.A. Raskovalov. Chaos, Solitons & Fractals **84**, 88 (2016).
[29] A.B. Borisov, Yu.A. Izyumov. Dokl. AN SSSR **283**, *4*, 859 (1985). (in Russian).
[30] T.H. Kim, S.H. Han, B.K. Cho. Commun. Phys. **2**, *1*, 41 (2019).
[31] I.T. Khabibullin. Theor. Math. Phys. **86**, *1*, 28 (1991).
[32] A.S. Fokas. Commun. Math. Phys. **230**, *1*, 1 (2002).
[33] E.K. Sklyanin. Func. Anal. Its. Appl. **21**, *2*, 164 (1987).
[34] P.N. Bibikov, V.O. Tarasov. Theor. Math. Phys. **79**, *3*, 570 (1989).
[35] A.S. Fokas. Physica D **35**, *1–2*, 167 (1989).
[36] V.V. Kiselev. JETP **136**, *3*, 330 (2023).
[37] V.V. Kiselev. Theor. Math. Phys. **219**, *1*, 576 (2024).
[38] V.V. Kiselev, A.A. Raskovalov. Bulletin of RUS **88**, *9*, 1382 (2024).
[39] V.V. Kiselev, A.A. Raskovalov. Chaos, Solitons & Fractals **188**, 115500 (2024).
[40] W.H. Meiklejohn, C.P. Bean. Phys. Rev. **102**, *5*, 1413 (1956).
[41] W.H. Meiklejohn, C.P. Bean. Phys. Rev. **105**, *3*, 904 (1957).
[42] B.N. Filippov. Mikromagnitnye struktury i ikh nelinejnye svojstva, Chast 1. UrO RAN, Ekaterinburg (2019). 423 s. (in Russian).
[43] J. Nogués, I.K. Schuller. J. Magn. Magn. Mater. **192**, *2*, 203 (1999).
[44] E.M. Lifshitz, L.P. Pitaevskii. Landau and Lifshitz Course of Theoretical Physics. Volume 9. Statistical Physics. Part 2. Elsevier Science (1995).
[45] A.I. Akhiezer, V.G. Baryakhtar, S.V. Peletminskiy. Spinovye volny. Nauka, M. (1967). 368 s. (in Russian).
[46] I.A. Akhiezer, A.E. Borovik. JETP **25**, *5*, 885 (1967).

Translated by I.Mazurov